

# Running interfacial waves in two-layer fluid system subject to longitudinal vibrations

D S Goldobin<sup>1,2,3</sup>, A V Pimenova<sup>1</sup>, K V Kovalevskaya<sup>1</sup>,  
D V Lyubimov<sup>2</sup> and T P Lyubimova<sup>1,2</sup>

<sup>1</sup> Institute of Continuous Media Mechanics, UB RAS, 1 Akademik Korolev street,  
Perm 614013, Russia

<sup>2</sup> Department of Theoretical Physics, Perm State University, 15 Bukireva str.,  
614990, Perm, Russia

<sup>3</sup> Department of Mathematics, University of Leicester, University Road, Leicester  
LE1 7RH, UK

E-mail: Denis.Goldobin@gmail.com

**Abstract.** We study the waves at the interface between two thin horizontal layers of immiscible fluids subject to high-frequency horizontal vibrations. Previously, the variational principle for energy functional, which can be adopted for treatment of quasi-stationary states of free interface in fluid dynamical systems subject to vibrations, revealed existence of standing periodic waves and solitons in this system. However, this approach does not provide regular means for dealing with evolutionary problems: neither stability problems nor ones associated with propagating waves. In this work, we rigorously derive the evolution equations for long waves in the system, which turn out to be identical to the ‘plus’ (or ‘good’) Boussinesq equation. With these equations one can find all time-independent-profile solitary waves (standing solitons are a specific case of these propagating waves), which exist below the linear instability threshold; the standing and slow solitons are always unstable while fast solitons are stable. Depending on initial perturbations, unstable solitons either grow in an explosive manner, which means layer rupture in a finite time, or falls apart into stable solitons. The results are derived within the long-wave approximation as the linear stability analysis for the flat-interface state [Lyubimov D V and Cherepanov A A 1987 *Fluid Dynamics* **21** 849–854] reveals the instabilities of thin layers to be long-wavelength.

Keywords: interfacial waves, two-layer fluid system, longitudinal vibrations, solitons, long waves

## 1. Introduction

In [1, 2] Wolf reported experimental observations of the occurrence of steady wave patterns on the interface between immiscible fluids subject to horizontal vibrations. The build-up of theoretical basis for these experimental findings was initiated with the linear instability analysis of the flat state of the interface [3, 4, 5] (see figure 1 for the sketch of the system considered in these works). Specifically, it was found that in thin layers the instability is a long-wavelength one [3]. In [4, 5], the linear stability was determined for the case of arbitrary frequency of vibrations.

In spite of the substantial advance in theoretical studies, the problem proved to require subtle approaches; a comprehensive straightforward weakly-nonlinear analysis of the system subject to high-frequency vibrations still remains lacking in the literature (as well as the long-wavelength one). The approach employed in [3] can be (and was) used for analysis of time-independent quasi-steady patterns (including non-linear ones) only, but not the evolution of these patterns over time. This “restricted” analysis of the system revealed that quasi-steady patterns can occur both via sub- and supercritical pitchfork bifurcations, depending on the system parameters. Later on, specifically for thin layers, which will be in focus of our work, the excitation of patterns was shown to be always subcritical [6] (paper [6] is published only in Russian, although the result can be derived from [3] as well). Within the approach of [3, 6] neither time-dependent patterns nor the stability of time-independent patterns can be analyzed. Specifically for the case of subcritical excitation, time-independent patterns may belong to the stability boundary between the attraction basins of the flat-interface state and the finite-amplitude pattern state in the phase space.<sup>‡</sup>

In this work we accomplish the task of derivation of the governing equations for dynamics of patterns on the interface of two-layer fluid system within the approximation of inviscid fluids. In Wolf’s experiments [1, 2], the viscous boundary layer in the most viscous liquid was an order of magnitude thinner than the liquid layer, meaning the approximation of inviscid liquid to be relevant. The layer is assumed to be thin enough for the evolving patterns to be long-wavelength [3]. With governing equations we analyze the dynamics of the system below the linear instability threshold, where the system turns out to be identical to the ‘plus’ Boussinesq equation. The system admits soliton solutions, these solutions are parameterized with single parameter, soliton speed. The maximal speed of solitons equals the minimal group velocity of linear waves in the system; the soliton waves move always slower than the packages of linear waves. Stability analysis reveals that the standing and slow solitons are unstable while fast solitons are stable. The system, as the ‘plus’ Boussinesq equation, is known to be fully integrable.

Recently, the problem of stability of a liquid film on a horizontal substrate subject to tangential vibrations was addressed in the literature [8]. The stability analysis for

<sup>‡</sup> In the idealistic dissipation-free case, when there are no attracting states, the basins of attraction are replaced with the basins of dynamics around corresponding states; i.e., of running perturbations around the flat-interface state and of evolving finite-amplitude patterns.

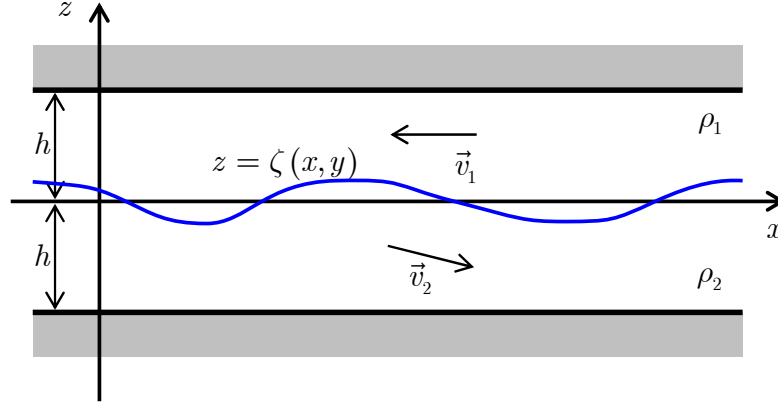


**Figure 1.** Sketch of a two-layer fluid system subject to longitudinal vibrations and the coordinate frame.

space-periodic patterns and solitary waves for the latter system was reported in [9]. The similarity of this problem with the problem we consider and expected similarity of results are illusive. Firstly, for the problem of [8] the liquid film is involved into oscillating motion only owing to viscosity, an inviscid liquid will be motionless over the tangentially vibrating substrate, while in the system we consider the inviscid fluid layers will oscillate owing to motion of the lateral boundaries of container and fluid incompressibility [3, 4, 5]. Secondly, the single-film case corresponds to the case of zero density of the upper layer in a two-layer system; in the system we consider this is a very specific case. These dissimilarities have their reflection in resulting mathematical models; the governing equations for long-wavelength patterns derived in [8] is of the 1st order with respect to time and the 4th order with respect to the space coordinate and describes purely dissipative patterns in viscous fluid, while the equation we will report is of 2nd order in time, 4th order in space and describes non-dissipative dynamics.

The paper is organized as follows. In Section 2 we provide physical description and mathematical model for the system under consideration. In Section 3 the governing equations for long-wavelength patterns are derived and discussed. In Section 4 soliton solutions are presented and their stability properties are analyzed. Conclusions are drawn in Section 5.

## 2. Problem statement and governing equations

We consider a system of two horizontal layers of immiscible inviscid fluids, confined between two impermeable horizontal boundaries (see figure 1). The system is subject to high-frequency longitudinal vibrations of linear polarization; the velocity of vibrational motion of the system is  $be^{i\omega t} + c.c.$  (here and hereafter, “*c.c.*” stands for complex conjugate). For simplicity, we consider the case of equal thickness, say  $h$ , of two layers,

which is not expected to change the qualitative picture of the system behavior [§] but makes calculations simpler. The density of upper liquid  $\rho_1$  is smaller than the density of the lower one  $\rho_2$ . We choose the horizontal coordinate  $x$  along the direction of vibrations, the  $z$ -axis is vertical with origin at the unperturbed interface between layers.

In this system, at the limit of infinitely extensive layers, the state with flat interface  $z = \zeta(x, y) = 0$  is always possible. If the layers are limited in horizontal directions by impermeable lateral boundaries, the interface will be nearly flat at a distance from these boundaries. For inviscid fluids, this state (the ground state) is featured by spatially homogeneous pulsating velocity fields  $\vec{v}_{j0}$  in both layers;

$$\vec{v}_{j0} = a_j(t)\vec{e}_x, \quad a_j(t) = A_j e^{i\omega t} + c.c., \quad A_1 = \frac{\rho_2 b}{\rho_1 + \rho_2}, \quad A_2 = \frac{\rho_1 b}{\rho_1 + \rho_2}, \quad (1)$$

where  $j = 1, 2$  and  $\vec{e}_x$  is the unit vector of the  $x$ -axis. (The time instant  $t = 0$  is chosen so that  $b$  and  $A_j$  are real.) The result (1) follows from the condition of zero pressure jump across the uninflected interface and the condition of the total fluid flux through the vertical cross-section being equal  $\int_{-h}^{+h} v^{(x)} dz = 2h(b e^{i\omega t} + c.c.)$  (which is due to the system motion with velocity  $b e^{i\omega t} + c.c.$ ).

Considering flow of inviscid fluid, it is convenient to introduce potential  $\phi_j$  of the velocity field;

$$\vec{v}_j = -\nabla \phi_j. \quad (2)$$

The mass conservation law for incompressible fluid,  $\nabla \cdot \vec{v}_j = 0$ , yields the Laplace equation for potential,  $\Delta \phi_j = 0$ . The kinematic conditions on the top and bottom boundaries

$$\phi_{1z}(z = h) = \phi_{2z}(z = -h) = 0 \quad (3)$$

and on the interface  $z = \zeta(x, y)$

$$\dot{\zeta} = -\phi_{1z} + \nabla \phi_1 \cdot \nabla \zeta, \quad (4)$$

$$\dot{\zeta} = -\phi_{2z} + \nabla \phi_2 \cdot \nabla \zeta \quad (5)$$

are also to be taken into account. (Here and hereafter, the upper dot stands for the time-derivative and letter in subscript denotes partial derivative with respect to the corresponding coordinate.) Equations (4) and (5) can be derived from the condition that the points of zero value of the distance function  $F = z - \zeta(x, y)$ , which correspond to the position of the interface, move with fluid, i.e., the Lagrangian derivative (material derivative)  $dF/dt = \partial F/\partial t + \vec{v} \cdot \nabla F$  is zero on the interface:  $-\dot{\zeta} + v^{(z)} - \vec{v} \cdot \nabla \zeta = 0$ , and this holds for both fluids.

After substitution of the potential flow, the Euler equation takes the following form:

$$\nabla \left( -\dot{\phi}_j + \frac{1}{2} (\nabla \phi_j)^2 \right) = \nabla \left( -\frac{1}{\rho_j} p_j - g z \right),$$

§ For problems considered in [3, 4, 5, 6], moderate discrepancies between two thicknesses resulted only in quantitative corrections.

where  $g$  is the gravity. The latter equation provides the expression for the pressure field in the volume of two fluids for a given flow field;

$$p_j = p_{j0} + \rho_j \left( \dot{\phi}_j - \frac{1}{2} (\nabla \phi_j)^2 - gz \right). \quad (6)$$

Now the stress on the interface is remaining to be brought into account to make the equation system self-contained by providing required boundary conditions for  $\phi_j$  on the interface between two fluids. The pressure jump across the interface is owned by the surface tension;

$$z = \zeta(x, y) : \quad p_1 - p_2 = -\alpha \nabla \cdot \vec{n} \quad \left( \text{where } \vec{n} := \frac{\nabla F}{|\nabla F|} \right), \quad (7)$$

where  $\alpha$  is the surface tension coefficient and  $\vec{n}$  is the unit vector normal to the interface.

The system we consider does not possess any internal instability mechanisms in the absence of vibrations (unlike, e.g., [10, 11]). Vibrations discriminate one of horizontal directions and there are no reasons to expect that close to the threshold of vibration-induced instabilities the excited patterns will experience spatial modulation along the  $y$ -direction, which is perpendicular to the vibration polarization direction. Furthermore, the linear stability analysis revealed the marginal vibration-induced instability of the flat-interface state to be long-wavelength [3, 6]. Hence, we restrict our consideration to the case of  $(x, z)$ -geometry and the long-wavelength approximation,  $|\partial_x \vec{v}| \ll |\partial_z \vec{v}|$ .

### 3. Governing equations for large-scale (long-wavelength) patterns

#### 3.1. Derivation of equations

In this section we derive the governing equation for long-wavelength patterns. We employ the standard multiscale method with small parameters  $\omega^{-1}$  and  $l^{-1}$ , where  $l$  is the reference horizontal length of patterns,  $\partial_x \sim l^{-1}$ . The hierarchy of small parameters and the orders of magnitude of fields will be established in the course of derivation.

Within the long-wavelength approximation, the solutions to the Laplace equation for  $\phi_j(x, t)$  satisfying boundary conditions (3) in the most general form read

$$\phi_1 = -a_1(t)x + \Phi_1(x, t) - \frac{1}{2}(h - z)^2 \Phi_{1xx}(x, t) + \frac{1}{4!}(h - z)^4 \Phi_{1xxxx}(x, t) - \dots, \quad (8)$$

$$\phi_2 = -a_2(t)x + \Phi_2(x, t) - \frac{1}{2}(h + z)^2 \Phi_{2xx}(x, t) + \frac{1}{4!}(h + z)^4 \Phi_{2xxxx}(x, t) - \dots. \quad (9)$$

Here the ground state (the flat-interface state) is represented by the terms  $-a_j(t)x$ ;  $\Phi_j(x, t)$  describe perturbation flow, they are yet arbitrary functions of  $x$  and  $t$ . After substitution of  $p_j$  from expression (6) and  $\phi_j$  from expressions (8)–(9), the condition of stress balance on the interface (7) reads

$$p_{1\infty} - p_{2\infty} + \rho_1 \left[ -\dot{a}_1 x + \dot{\Phi}_1 - \frac{(h - \zeta)^2}{2} \dot{\Phi}_{1xx} \right]$$

$$\begin{aligned}
& -\frac{1}{2} \left( -a_1 + \Phi_{1x} - \frac{(h-\zeta)^2}{2} \Phi_{1xxx} \right)^2 - \frac{((h-\zeta)\Phi_{1xx})^2}{2} + \dots \Big] \\
& - \rho_2 \left[ -\dot{a}_2 x + \dot{\Phi}_2 - \frac{(h+\zeta)^2}{2} \dot{\Phi}_{2xx} \right. \\
& \quad \left. - \frac{1}{2} \left( -a_2 + \Phi_{2x} - \frac{(h+\zeta)^2}{2} \Phi_{2xxx} \right)^2 - \frac{((h+\zeta)\Phi_{2xx})^2}{2} + \dots \right] \\
& + (\rho_2 - \rho_1)g\zeta = \alpha \frac{\zeta_{xx}}{(1 + \zeta_x^2)^{3/2}}.
\end{aligned}$$

Here “...” stand for terms  $\mathcal{O}_1(\dot{\Phi}_j h^4/l^4) + \mathcal{O}_2(a_j \Phi_j h^4/l^5) + \mathcal{O}_3(\Phi_j^2 h^4/l^6)$ . The difference of constants  $p_{1\infty} - p_{2\infty}$  is to be determined from the condition that in the area of vanishing perturbations of the pulsation flow, i.e.  $\Phi_j(x, t) = \text{const}$ , the interface remains aflat, i.e.  $\zeta(x, t) = 0$ . This condition yields  $p_{1\infty} - p_{2\infty} - (\rho_1 a_1^2(t) - \rho_2 a_2^2(t))/2 = 0$ . Choosing measure units for length:  $L = \sqrt{\alpha/[(\rho_2 - \rho_1)g]}$ , for time:  $T = L/b$ , and for the fluid densities:  $\rho_*$ —which means replacement

$$\begin{aligned}
(x, z) & \rightarrow (Lx, Lz), \quad t \rightarrow Tt, \quad \zeta \rightarrow L\zeta, \\
\Phi_j & \rightarrow (L^2/T)\Phi_j, \quad \rho_i \rightarrow \rho_* \rho_i
\end{aligned} \tag{10}$$

in equations—one can rewrite the last equation in the dimensionless form

$$\begin{aligned}
B \Big[ & \frac{\rho_1 a_1^2 - \rho_2 a_2^2}{2} + \rho_1 \dot{\Phi}_1 - \rho_2 \dot{\Phi}_2 - \frac{\rho_1 (h-\zeta)^2}{2} \dot{\Phi}_{1xx} + \frac{\rho_2 (h+\zeta)^2}{2} \dot{\Phi}_{2xx} \\
& - \frac{\rho_1}{2} \left( a_1 - \Phi_{1x} + \frac{1}{2} (h-\zeta)^2 \Phi_{1xxx} \right)^2 \\
& + \frac{\rho_2}{2} \left( a_2 - \Phi_{2x} + \frac{1}{2} (h+\zeta)^2 \Phi_{2xxx} \right)^2 \\
& - \frac{\rho_1}{2} ((h-\zeta)\Phi_{1xx})^2 + \frac{\rho_2}{2} ((h+\zeta)\Phi_{2xx})^2 + \dots \Big] + \zeta = \frac{\zeta_{xx}}{(1 + \zeta_x^2)^{3/2}}.
\end{aligned} \tag{11}$$

Here the dimensionless vibration parameter

$$B \equiv \frac{\rho_* b^2}{\sqrt{\alpha(\rho_2 - \rho_1)g}} = B_0 + B_1 \tag{12}$$

( $\rho_j$  is dimensional here), where  $B_0$  is the critical value of the vibration parameter above which the flat-interface state becomes linearly unstable,  $B_1$  is a small deviation of the vibration parameter from the critical value. Further, kinematic conditions (4) and (5) turn into

$$\dot{\zeta} = \left( -(h-\zeta)\Phi_{1x} + \frac{1}{3!} h^3 \Phi_{1xxx} - a_1 \zeta + \dots \right)_x, \tag{13}$$

$$\dot{\zeta} = \left( (h+\zeta)\Phi_{2x} - \frac{1}{3!} h^3 \Phi_{2xxx} - a_2 \zeta + \dots \right)_x. \tag{14}$$

Here “...” stand for  $\mathcal{O}_1(\Phi_j h^2 \zeta / l^3) + \mathcal{O}_2(\Phi_j h^4 / l^5)$ . Equations (11), (13) and (14) form a self-contained equation system.

It is convenient to distinguish two main time-modes in fields: the average over vibration period part and the pulsation part;

$$\zeta = \eta(\tau, x) + \xi(\tau, x)e^{i\omega t} + c.c. + \dots,$$

$$\Phi_j = \varphi_j(\tau, x) + \psi_j(\tau, x)e^{i\omega t} + c.c. + \dots,$$

where  $\tau$  is a “slow” time related to the average over vibration period evolution and “...” stand for higher powers of  $e^{i\omega t}$ .

In order to develop expansion in small parameter  $\omega^{-1}$ , we have to adopt certain hierarchy of smallness of parameters, fields, etc. We adopt small deviation from the instability threshold  $B_1 \sim \omega^{-1}$ . Then  $\eta \sim \omega^{-1}$  and  $\partial_x \sim \omega^{-1/2}$  (cf. [3, 6]). It is as well established (e.g., [3, 6]) that for finite wavelength perturbations (finite  $k \neq 0$ )  $B_0(k) = B_0(0) + Ck^2 + \mathcal{O}(k^4)$ . Generally, the expansion of exponential growth rate of perturbations in series of  $B_1$  near the instability threshold possesses a non-zero linear part, and  $B_0(k) - B_0(0) \sim k^2$ ; therefore,  $\partial_\tau \sim \mathcal{O}_1(B_1) + \mathcal{O}_2(k^2) \sim \omega^{-1}$ . The order of magnitude of  $\xi$ ,  $\varphi_j$  and  $\psi_j$  is more convenient to be determined in the course of development of the expansion.

Collecting in equations (13) and (14) terms with  $e^{i\omega t}$ , one finds

$$i\omega\xi + \xi_\tau = \left( -(h - \eta)\psi_{1x} + \frac{1}{3!}h^3\psi_{1xxx} + \xi\varphi_{1x} - A_1\eta + \dots \right)_x, \quad (15)$$

$$i\omega\xi + \xi_\tau = \left( (h + \eta)\psi_{2x} - \frac{1}{3!}h^3\psi_{2xxx} + \xi\varphi_{2x} - A_2\eta + \dots \right)_x, \quad (16)$$

where “...” stand for  $\mathcal{O}_1((\xi\varphi + \eta\psi)h^2/l^4) + \mathcal{O}_2(\psi h^4/l^6)$ . Constant with respect to  $t$  terms sum-up to

$$\eta_\tau = \left( -(h - \eta)\varphi_{1x} + \xi\psi_{1x}^* + c.c. - A_1\xi^* + c.c. + \dots \right)_x, \quad (17)$$

$$\eta_\tau = \left( (h + \eta)\varphi_{2x} + \xi\psi_{2x}^* + c.c. - A_2\xi^* + c.c. + \dots \right)_x, \quad (18)$$

where the superscript “\*” stands for complex conjugate and “...” stand for  $\mathcal{O}_1((\eta\varphi + \xi\psi)h^2/l^4) + \mathcal{O}_2(\varphi h^4/l^6)$ . The difference of equations (15) and (16) yields  $\psi_j \sim \omega^{-1/2}$ , and the difference of (17) and (18) yields  $\varphi_j \sim \omega^{-1}$ . For dealing with non-linear terms in the consideration that follows, it is convenient to extract the first correction to  $\psi_j$  explicitly, i.e. write  $\psi_j = \psi_j^{(0)} + \psi_j^{(1)} + \dots$ , where  $\psi_j^{(1)} \sim \omega^{-1}\psi_j^{(0)} \sim \omega^{-3/2}$ . Equation (15) (or (16)) yields in the leading order ( $\sim \omega^{-3/2}$ )

$$\xi = \frac{i}{\omega}(h\psi_{1x} + A_1\eta)_x \sim \omega^{-5/2}. \quad (19)$$

Considering the difference of (16) and (15), one has to keep in mind, that we are interested in localized patterns for which  $\Phi_{jx}(x = \pm\infty) = 0$ ,  $\zeta(x = \pm\infty) = 0$ . Hence, this difference can be integrated with respect to  $x$ , taking the form

$$h(\psi_1 + \psi_2)_x - \eta(\psi_1 - \psi_2)_x - \frac{1}{6}h^3(\psi_1 + \psi_2)_{xxx} - \xi(\varphi_1 - \varphi_2)_x + (A_1 - A_2)\eta + \dots = 0,$$

which yields in the first two orders of smallness

$$h(\psi_1^{(0)} + \psi_2^{(0)})_x = -(A_1 - A_2)\eta = -\frac{\rho_2 - \rho_1}{\rho_2 + \rho_1}\eta, \quad (20)$$

$$h(\psi_1^{(1)} + \psi_2^{(1)})_x = (\psi_1^{(0)} - \psi_2^{(0)})_x \eta + \frac{1}{6}h^3(\psi_1^{(0)} + \psi_2^{(0)})_{xxx}. \quad (21)$$

The difference and the sum of equations (17) and (18) yield in the leading order, respectively,

$$\varphi_1 = -\varphi_2 \equiv \varphi, \quad (22)$$

$$\eta_\tau = -h\varphi_{xx}. \quad (23)$$

Let us now consider equation (11). We will collect groups of terms with respect to power of  $e^{i\omega t}$  and the order of smallness in  $\omega^{-1}$ .

$\sim \omega^{+\frac{1}{2}}e^{i\omega t}$ :

$$i\omega B_0(\rho_1\psi_1^{(0)} - \rho_2\psi_2^{(0)}) = 0.$$

We introduce

$$\psi^{(0)} \equiv \rho_j \psi_j^{(0)}. \quad (24)$$

The last equation and equation (20) yield

$$\psi_x^{(0)} = -\frac{1}{h} \frac{\rho_1 \rho_2 (\rho_2 - \rho_1)}{(\rho_2 + \rho_1)^2} \eta. \quad (25)$$

$\sim \omega^0 e^{i\omega t}$ :

No contributions.

$\sim \omega^{-\frac{1}{2}} e^{i\omega t}$ :

$$\begin{aligned} & i\omega B_1 \underbrace{(\rho_1 \psi_1^{(0)} - \rho_2 \psi_2^{(0)})}_{=0} + i\omega B_0 (\rho_1 \psi_1^{(1)} - \rho_2 \psi_2^{(1)}) \\ & + B_0 \underbrace{(\rho_1 \psi_1^{(0)} - \rho_2 \psi_2^{(0)})_\tau}_{=0} + i\omega B_0 \frac{h^2}{2} \underbrace{(\rho_2 \psi_{2xx}^{(0)} - \rho_1 \psi_{1xx}^{(0)})}_{=0} = 0. \end{aligned}$$

(We marked the combinations which are known to be zero from the leading order of expansion.) Similarly to (24), we introduce

$$\psi^{(1)} \equiv \rho_j \psi_j^{(1)}. \quad (26)$$

The last equation and equation (21) yield

$$\begin{aligned} \psi_x^{(1)} &= \frac{1}{h} \frac{\rho_2 - \rho_1}{\rho_2 + \rho_1} \psi_x^{(0)} \eta + \frac{h^2}{6} \psi_{xxx}^{(0)} \\ &= -\frac{\rho_1 \rho_2 (\rho_2 - \rho_1)^2}{h^2 (\rho_2 + \rho_1)^3} \eta - \frac{h \rho_1 \rho_2 (\rho_2 - \rho_1)}{6 (\rho_2 + \rho_1)^2} \eta_{xx}. \end{aligned} \quad (27)$$

$\sim \omega^{-1} (e^{i\omega t})^0$ :

$$B_0[-\rho_2(A_2\psi_{2x}^{(0)*} + c.c.) + \rho_1(A_1\psi_{1x}^{(0)*} + c.c.)] + \eta = 0.$$



With substitutions (24) and (25) the last equation takes form

$$\left[ -\frac{2B_0\rho_1\rho_2(\rho_2 - \rho_1)^2}{h(\rho_2 + \rho_1)^3} + 1 \right] \eta = 0.$$

Thus we obtain the solvability condition, which poses a restriction on  $B_0$ ; this restriction determines the linear instability threshold

$$B_0 = \frac{(\rho_2 + \rho_1)^3 h}{2\rho_1\rho_2(\rho_2 - \rho_1)^2}. \quad (28)$$

$\sim \omega^{-2}(e^{i\omega t})^0$ : (using (22) for  $\varphi_j$ )

$$\begin{aligned} & B_1 \underbrace{[-\rho_2(A_2\psi_{2x}^{(0)*} + c.c.) + \rho_1(A_1\psi_{1x}^{(0)*} + c.c.)]}_{=-\eta/B_0} \\ & + B_0 \left[ (\rho_2 + \rho_1)\varphi_\tau + \rho_2|\psi_{2x}^{(0)}|^2 - \rho_2 \left( A_2\psi_{2x}^{(1)*} + c.c. - A_2\frac{h^2}{2}\psi_{2xxx}^{(0)*} + c.c. \right) \right. \\ & \left. - \rho_1|\psi_{1x}^{(0)}|^2 + \rho_1 \left( A_1\psi_{1x}^{(1)*} + c.c. - A_1\frac{h^2}{2}\psi_{1xxx}^{(0)*} + c.c. \right) \right] = \eta_{xx}. \end{aligned}$$

Substituting  $\psi_j^{(n)}$  from (24)–(27), one can rewrite the last equation as

$$\begin{aligned} & -\frac{B_1}{B_0}\eta + B_0 \left[ (\rho_2 + \rho_1)\varphi_\tau - \frac{\rho_2 - \rho_1}{\rho_2\rho_1} \left( \frac{\rho_1\rho_2(\rho_2 - \rho_1)}{h(\rho_2 + \rho_1)^2} \right)^2 \eta^2 - \frac{2\rho_1\rho_2(\rho_2 - \rho_1)^3}{h^2(\rho_2 + \rho_1)^4} \eta^2 \right. \\ & \left. - \frac{h\rho_1\rho_2(\rho_2 - \rho_1)^2}{3(\rho_2 + \rho_1)^3} \eta_{xx} + h^2 \frac{\rho_1\rho_2(\rho_2 - \rho_1)^2}{h(\rho_2 + \rho_1)^3} \eta_{xx} \right] = \eta_{xx}. \end{aligned}$$

Together with equation (23) the latter equation form the final *system of governing equations for long-wavelength perturbations* of the flat-interface state:

$$\begin{cases} B_0(\tilde{\rho}_2 + \tilde{\rho}_1)\tilde{\varphi}_{\tilde{\tau}} = \left[ 1 - \frac{\tilde{h}^2}{3} \right] \tilde{\eta}_{\tilde{x}\tilde{x}} + \frac{3}{2\tilde{h}} \frac{\tilde{\rho}_2 - \tilde{\rho}_1}{\tilde{\rho}_2 + \tilde{\rho}_1} \tilde{\eta}^2 + \frac{B_1}{B_0} \tilde{\eta}, \\ \tilde{\eta}_{\tilde{\tau}} = -\tilde{h} \tilde{\varphi}_{\tilde{x}\tilde{x}}. \end{cases} \quad (29)$$

Here we explicitly mark the dimensionless variables and parameters with the tilde sign to distinguish them from original dimensional variables and parameters. Above in this paragraph, the tilde sing was omitted to make calculations possibly less laborious. For convenience we explicitly specify how to read rescaling (10) with the tilde-notation:  $x = L\tilde{x}$ ,  $t = (L/b)\tilde{t}$ ,  $\rho_i = \rho_*\tilde{\rho}_i$ , etc. The expression for  $B_0$  (28) in original dimensional terms reads

$$B_0 = \frac{\rho_*(\rho_2 + \rho_1)^3 h}{2\rho_1\rho_2(\rho_2 - \rho_1)^2} \sqrt{\frac{(\rho_2 - \rho_1)g}{\alpha}}. \quad (30)$$

Notice, equation system (29) is valid for  $B_1$  small compared to  $B_0$ , otherwise one cannot stay within the long-wavelength approximation. Rarely, it is possible to use long-wavelength for finite deviations from the linear instability threshold and derive certain information on the system dynamics (e.g., in [14] for Soret-driven convection from localized sources of heat or solute in a thin porous layer, an unavoidable appearance of patterns similar to hydraulic jumps [15] was predicted within the long-wavelength approximation though for a finite deviation from the linear instability threshold).

### 3.2. On the long-wavelength character of the linear instability

In the text above, we relied on the fact that instability is long-wavelength for thin enough layers. Now we have appropriate quantifiers to specify quantitatively, what means “thin enough”. According to [3], it requites  $\tilde{h} < \sqrt{3}$ . Remarkably, we can see a footprint of this fact from equation system (29) with multiplier  $[1 - \tilde{h}^2/3]$  ahead of  $\tilde{\eta}_{\tilde{x}\tilde{x}}$ . Indeed, the exponential growth rate  $\tilde{\lambda}$  of linear normal perturbations  $(\tilde{\eta}, \tilde{\varphi}) \propto \exp(\tilde{\lambda}\tilde{t} + i\tilde{k}\tilde{x})$  of the trivial state obeys

$$\tilde{\lambda}^2 = \frac{\tilde{h} \tilde{k}^2}{B_0(\tilde{\rho}_2 + \tilde{\rho}_1)} \left( - \left[ 1 - \frac{\tilde{h}^2}{3} \right] \tilde{k}^2 + \frac{B_1}{B_0} \right). \quad (31)$$

Below the linear instability threshold of infinitely long wavelength perturbations, i.e. for  $B_1 < 0$ , there are no growing perturbations for  $\tilde{h} < \sqrt{3}$ , while the perturbations with large enough  $\tilde{k}$  grow for  $\tilde{h} > \sqrt{3}$ . Of course, this analysis of equation system (29) only highlights the long-wavelength character of the linear instability, since it deals with the limit of small  $\tilde{k}$  and does not provide information on the linear stability for finite  $\tilde{k}$ . A comprehensive proof of the long-wavelength character of the instability for  $\tilde{h} < \sqrt{3}$  comes from [3].

In the following we will consider the system behavior below the linear instability threshold, i.e. for negative  $B_1$ . It is convenient to make further rescaling of coordinates and variables:

$$\begin{aligned} \tilde{x} &\rightarrow x \sqrt{\frac{B_0}{(-B_1)} \left[ 1 - \frac{\tilde{h}^2}{3} \right]}, & \tilde{t} &\rightarrow t \sqrt{\frac{\tilde{\rho}_2 - \tilde{\rho}_1}{\tilde{h}} \frac{B_0^3}{B_1^2} \left[ 1 - \frac{\tilde{h}^2}{3} \right]}, \\ \tilde{\eta} &\rightarrow \eta \tilde{h} \frac{\tilde{\rho}_2 + \tilde{\rho}_1}{\tilde{\rho}_2 - \tilde{\rho}_1} \frac{(-B_1)}{B_0}, & \tilde{\varphi} &\rightarrow \varphi \sqrt{\frac{(\tilde{\rho}_2 + \tilde{\rho}_1)^2}{(\tilde{\rho}_2 - \tilde{\rho}_1)^3} \frac{B_1^2}{\tilde{h} B_0^3} \left[ 1 - \frac{\tilde{h}^2}{3} \right]}. \end{aligned} \quad (32)$$

Notice, that this means the following rescaling of *initial dimensional* coordinates and variables:

$$\begin{aligned} x &\rightarrow x L \sqrt{\frac{B_0}{(-B_1)} \left[ 1 - \frac{h^2}{3L^2} \right]}, & t &\rightarrow t \sqrt{\frac{\rho_2 - \rho_1}{\rho_*} \frac{L^3 B_0^3}{h b^2 B_1^2} \left[ 1 - \frac{h^2}{3L^2} \right]}, \\ \eta &\rightarrow \eta h \frac{\rho_2 + \rho_1}{\rho_2 - \rho_1} \frac{(-B_1)}{B_0}, & \varphi &\rightarrow \varphi \sqrt{\frac{\rho_*(\rho_2 + \rho_1)^2}{(\rho_2 - \rho_1)^3} \frac{L^3 B_1^2}{h b^2 B_0^3} \left[ 1 - \frac{h^2}{3L^2} \right]}. \end{aligned} \quad (33)$$

After this rescaling equation system (29) takes zero-parametric form;

$$\dot{\varphi} = \eta_{xx} + \frac{3}{2}\eta^2 - \eta, \quad (34)$$

$$\dot{\eta} = -\varphi_{xx}. \quad (35)$$

The derivation of the latter equation system itself is one of the main results we report with this paper, as it allows considering the evolution of quasi-steady patterns in the two-layer fluid system under the action of the vibration field.

### 3.3. The ‘plus’ Boussinesq equation and the original Boussinesq equation for gravity waves in shallow water

The equation system (34)–(35) can be rewritten in the form of a ‘plus’ Boussinesq equation (plus BE);

$$\ddot{\eta} - \eta_{xx} + \left( \frac{3}{2} \eta^2 + \eta_{xx} \right)_{xx} = 0. \quad (36)$$

Meanwhile, the original Boussinesq equation B (BE B) for gravity waves in a shallow water layer [16] or in a two-layer system without vibrations [17] reads

$$\ddot{\eta} - \eta_{xx} - \left( \frac{3}{2} \eta^2 + \eta_{xx} \right)_{xx} = 0. \quad (37)$$

Both systems are fully integrable and multi-solitons solutions are known for them from literature (e.g., [18, 19, 20]). However, their dynamics is essentially different; the original BE B suffers from the short-wave instability, while the plus BE is free from this instability. Solitons in the plus BE can be unstable, decaying into pairs of stable solitons or experiencing explosive formation of sharp peaks in finite time [20, 21, 22]. In the sections below we will provide overview of the soliton dynamics for equation (36) in relation to the fluid dynamical system we deal with. Prior to doing so, in this subsection, we would like to focus more on discussion of different kinds of the generalized Boussinesq equation and their relationships with dynamics of systems of fluid layers.

Small-amplitude gravity waves in shallow water are governed by the set A Boussinesq equations (equation system (25) in [16]) which read in our terms after proper rescaling as

$$\begin{cases} \dot{\eta} + \varphi_{xx} = -(\eta \varphi_x)_x + \frac{1}{6} \varphi_{xxxx}, \\ \dot{\varphi} + \eta = -\frac{1}{2} (\varphi_x)^2 + \frac{1}{2} \dot{\varphi}_{xx}, \end{cases} \quad (38)$$

where the terms in the right hand side of equations are small, i.e., both nonlinearity and dispersion are small. To the leading corrections owned by nonlinearity and dispersion, the latter equation system can be recast as

$$\ddot{\eta} - \eta_{xx} = \left( (\varphi_x)^2 + \frac{1}{2} \eta^2 + \eta_{xx} \right)_{xx}, \quad (39)$$

where small terms are collected in the r.h.s. part of the equation. For waves propagating in one direction  $\partial_x \approx \pm \partial_t$  and, to the leading corrections, one can make substitution  $(\varphi_x)^2 \approx (\dot{\varphi})^2 \approx \eta$ , which yields equation (37). Thus, the Boussinesq equation for the classical problem of waves in shallow water is not only inaccurate far from the edge of the spectrum of soliton speed (near  $c = 1$ ) but is also inappropriate for consideration of collisions of counterpropagating waves (as  $|\varphi_x| \neq |\dot{\varphi}|$  for them). On the contrast, the equations we derived for our physical system are accurate close to the vibration-induced instability threshold for the entire range of soliton speeds and all kinds of soliton interactions as long as the profile remains smooth.

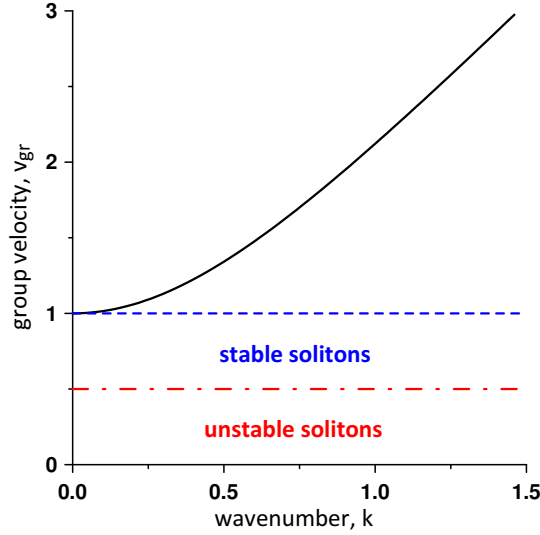


**Figure 2.** Group velocity  $v_{\text{gr}}$  of linear waves (black solid line) vs the wavenumber  $k$ . The group velocity for all wave packages is larger than the maximal soliton propagation velocity  $c = 1$ . (Soliton stability is discussed in the text below.)

It is also noteworthy, that character of the original Boussinesq equation B is inherent to the dynamics of inviscid fluid layers in force fields and does not change without special external fields, the action of which cannot be formally represented by any correction to the gravity. The case of vibration field turns out to be such one and yields the dynamics governed by the plus BE.

#### 4. Long waves below the linear instability threshold

In this section we consider waves in the dynamic system (34)–(35). In equations (33), one can see how the rescaling of each coordinate and variable depends on  $(-B_1) = B_0 - B$ . From these dependencies it can be seen, that for patterns in dynamic system (34)–(35) the corresponding patterns in real time–space will obey the following scaling behavior near the linear instability threshold: spatial extent  $x_* \propto 1/\sqrt{B_0 - B}$ , reference time  $t_* \propto 1/(B_0 - B)$ , reference profile deviation  $\eta_* \propto (B_0 - B)$ .

##### 4.1. Linear waves: dispersion equation, group velocity

Let us first describe propagation of small perturbations, linear waves, in dynamic system (34)–(35). For normal perturbations  $(\eta, \varphi) \propto \exp(-i\Omega t + ikx)$  the oscillation frequency reads

$$\Omega(k) = k\sqrt{1 + k^2}. \quad (40)$$

The corresponding phase velocity is

$$v_{\text{ph}} = \Omega/k = \sqrt{1 + k^2}, \quad (41)$$

and the group velocity, which describes propagation of envelopes of wave packages, is

$$v_{\text{gr}} = \frac{d\Omega}{dk} = \frac{1 + 2k^2}{\sqrt{1 + k^2}}. \quad (42)$$

One can see, the minimal group velocity to be 1 and the group velocity  $v_{\text{gr}}$  monotonously increases as wavelength decreases (see figure 2).

#### 4.2. Solitons

The dynamic system (34)–(35) admits time-independent-profile solutions, solitons  $\eta(x, t) = \eta(x - ct)$ , where  $c$  is the soliton velocity. With identical equality  $\partial_t \eta(x - ct) = -c \partial_x \eta(x - ct)$ , for localized patterns, which vanish at  $x \rightarrow \pm\infty$ , equation (35) can be once integrated and yields  $\varphi' = c\eta$  (here the prime denotes the differentiation with respect to argument). Equation (34) takes the form

$$0 = \eta'' + \frac{3}{2}\eta^2 - (1 - c^2)\eta. \quad (43)$$

The latter equation admits the soliton solution

$$\eta_0(x, t) = \frac{1 - c^2}{\cosh^2 \frac{\sqrt{1 - c^2}(x \pm ct)}{2}}, \quad (44)$$

the propagation direction ( $+c$  or  $-c$ ) is determined by the flow,  $\varphi' = \pm c\eta$ . The family of soliton solutions turns out to be one-parametric, parameterized by the speed  $c$  only. Speed  $c$  varies within the range  $[0, 1]$ ; standing soliton ( $c = 0$ ) is the sharpest and the highest one and for the fastest solitons,  $c \rightarrow 1$ , the spatial extent tends to infinity, while the height tends to 0.

Considering in the same way a non-rescaled equation system (29), one can see, that for a given physical system with vibration parameter  $B$  as a control parameter, the shape of a soliton solution is controlled by combination

$$[(-B_1)/B_0 - \tilde{c}^2 \tilde{h}^{-1} B_0 (\tilde{\rho}_2 + \tilde{\rho}_1)]. \quad (45)$$

This means that one and the same interface inflection soliton can exist for different values of  $B$ , though, since the shape-controlling parameter (45) should be the same, the non-rescaled soliton run speed  $\tilde{c}$  grows as the departure from the threshold  $(-B_1)$  increases.

Since  $v_{\text{gr}} \geq 1$  (see figure 2) and  $c^2 \leq 1$ , solitons of arbitrary height travel slower than any small perturbations of the flat-interface state. The maximal speed of solitons,  $c_{\text{max}} = 1$ , coincides with the minimal group velocity of linear waves. This yields noticeable information on the system dynamics. Fast solitons with  $c$  tending to 1 from below are extend and have a small height (see equation (44)), while envelopes of long linear waves propagate with velocity  $v_{\text{gr}}$  tending to 1 from above. This means that envelopes of small-height soliton packages travel faster than solitons in these packages.[||]

|| The issue of the generality of situations where the ranges of the possible soliton velocities and the group velocities of linear waves do not overlap but only touch each other is interestingly addressed in [12, 13] from the view point of emission of wave packages by the soliton (or impossibility of such an emission).

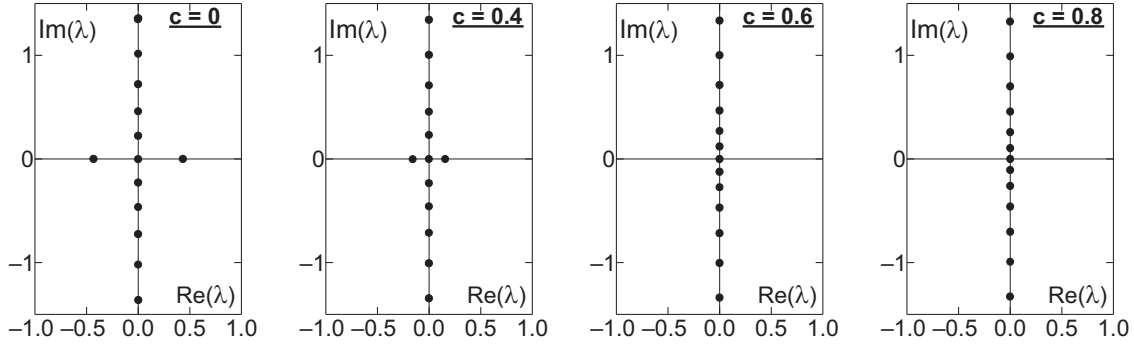


**Figure 3.** Spectra of eigenvalues  $\lambda$  of the problem (46)–(48) of linear stability of solitons with speed  $c$  specified in plots. The real part of  $\lambda$  is the exponential growth rate of perturbations; for  $c = 0$  and  $c = 0.4$ , one can see existence of one mode with positive  $\text{Re}(\lambda)$ , i.e. instability mode, while for  $c = 0.6$  and  $c = 0.8$ , all the perturbations oscillate without growth. In figure 4(b), the instability mode and the Goldstone mode of neutral stability (invariance to the shifts of soliton in space) are plotted for  $c = 0$ .

#### 4.3. Stability of solitons

The stability properties of solitons in the ‘plus’ Boussinesq equation were addressed in literature [19, 21, 22]; in [21] the solitons with  $1/2 \leq c \leq 1$  were proofed to be stable and in [22] the solitons with  $c < 1/2$  were proofed to be unstable. One can add more subtle details to this information: the spectrum of Lyapunov exponents (exponential growth rate) and the dependence of the scenario of nonlinear growth of perturbations on the initial perturbation.

The problem of linear stability of the soliton  $\eta_0(x - ct)$  to perturbations  $(e^{\lambda t}\eta_1(x_1), e^{\lambda t}\varphi_1(x_1))$  in the copropagating reference frame  $x_1 = x - ct$  reads

$$\lambda\varphi_1 + c\varphi_1' = \eta_1'' + 3\eta_0(x_1)\eta_1 - \eta_1, \quad (46)$$

$$\lambda\eta_1 + c\eta_1' = -\varphi_1'' \quad (47)$$

with boundary conditions

$$\eta_1(\pm\infty) = \varphi_1(\pm\infty) = 0. \quad (48)$$

The eigenvalue problem (46)–(48) was solved numerically with employment of the shooting method. The spectra of eigenvalues  $\lambda$  for different  $c$  are plotted in figure 3 and the first two eigenmodes of perturbations of the standing soliton ( $c = 0$ ) are plotted in figure 4(b). In figure 4(a), one can see the exponential growth rate  $\text{Re}(\lambda)$  of perturbations; the standing and slow solitons with  $c < 0.5$  are unstable, while the fast solitons with  $c \geq 0.5$  are stable.

The scenarios of evolution of unstable solitons were observed numerically by means of direct numerical simulation of the dynamic system (34)–(35) with the finite difference method in the  $x$ -domain of length 200 with periodic boundary conditions and the space step size  $h_x = 0.05$ .<sup>¶</sup> As in [18, 19, 20], two possible scenarios were observed: (i) soliton explosion with formation of a finite amplitude relief or, possibly, layer rupture;

<sup>¶</sup> The fact, that unperturbed unstable analytical solution used as initial conditions could persist for

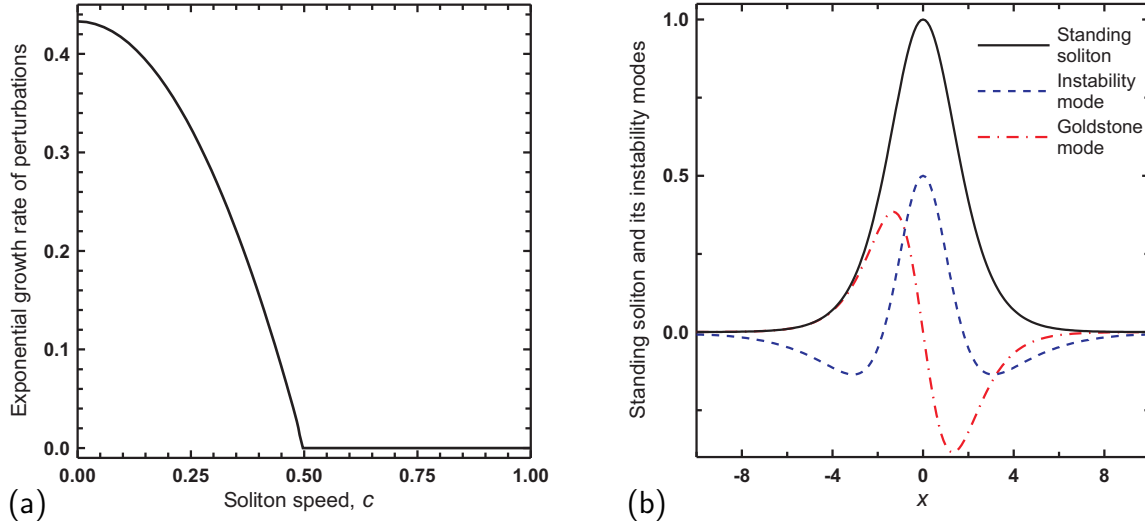


**Figure 4.** (a): Exponential growth rate  $\text{Re}(\lambda)$  of perturbations of soliton as a function of the soliton speed  $c$ . (b): The instability mode and the Goldstone mode of neutral stability (invariance to the shifts of soliton in space) of the standing soliton ( $c = 0$ ).

(ii) falling-apart of the soliton into two stable solitons (figure 5). Since the phase space of the system is infinitely dimensional, the problem of discrimination of the initial perturbations leading to explosion and those leading to falling-apart may be generally nontrivial. However, in figure 3 one can see that there is only one instability mode for  $c < 1/2$  and the nonlinear evolution of perturbations turns out to depend only on projection of the small initial perturbation on this unstable direction. If the instability mode is normalized in such a way that  $\eta_1(x_1 = 0) > 0$  (cf. figure 4(b)), the initial perturbations with a positive scalar product with the instability mode lead to explosion, while the perturbations with a negative scalar product lead to falling-apart into two stable solitons.

## 5. Conclusion

We have considered the dynamics of patterns on the internal surface of the horizontal two-layer system of inviscid fluids subject to tangential vibrations. For thin layers ( $h < \sqrt{3\alpha/[(\rho_2 - \rho_1)g]}$ ) we consider the instability is known to be long-wavelength and subcritical [3, 6]. Governing equations for long-wavelength patterns below the linear instability threshold have been derived—equation system (34)–(35)—allowing for the first time theoretical analysis for time-dependent patterns in the system and for stability of time-independent (quasi-steady) patterns. Noteworthy, the stability analysis for the only time-independent localized patterns in the system, standing solitons, have revealed them to be unstable.

The system dynamics is found to be governed by dynamic system (34)–(35) which up to 100 time units, suggests the discretisation and numerical integration schemes introduce quite a small inaccuracy into the system simulation.

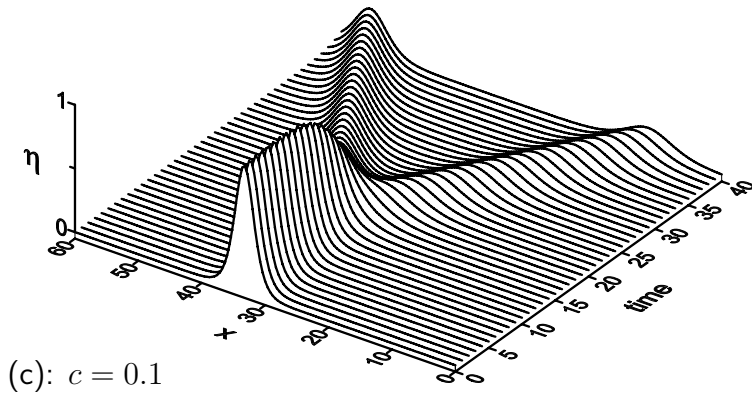
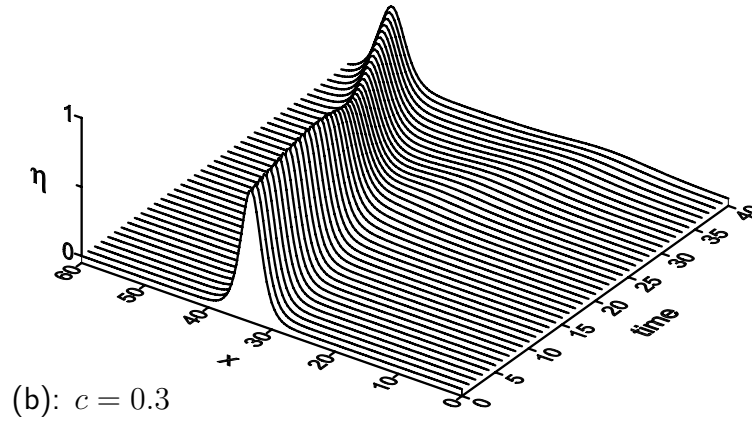
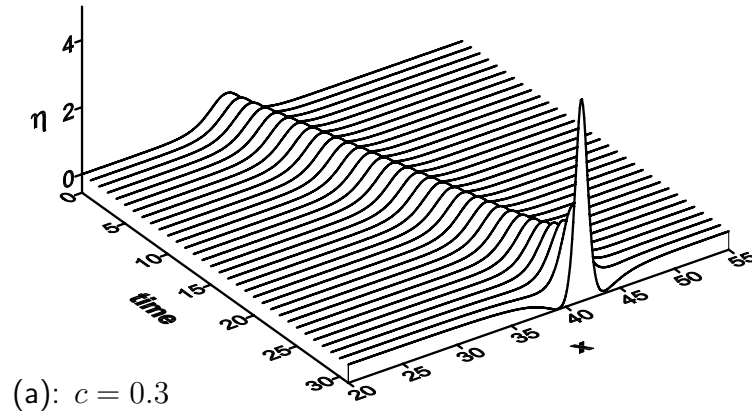


**Figure 5.** (a): The unstable soliton (44) of  $c = 0.3$  with tiny positive perturbation explodes leading to the formation of a finite amplitude relief, possibly layer rupture. (b): The same unstable soliton ( $c = 0.3$ ) with tiny negative perturbation falls apart into two fast stable solitons. (c): Falling-apart of the unstable soliton with  $c = 0.1$ .

is equivalent to the ‘plus’ Boussinesq equation. For dynamic system (34)–(35), one-parametric family of localized solutions of time-independent profile, solitons, exists (equation (44)). These solitons are up-standing embossments of the interface (cf. black curve in figure 4(b)) and parameterized by the soliton speed  $c$  only, which varies from  $c = 0$  (the highest and sharpest solitons) to  $c = 1$  (solitons with width tending to infinity



and height tending to zero). The standing and slow solitons ( $c < 1/2$ ) are unstable [22], while the fast solitons ( $c \geq 1/2$ ) are stable [21]. The group velocity of linear waves in the system is  $v_{gr} \geq 1$ , meaning all the solitons to travel slower than any wave packages of small perturbations of the flat-interface state.

Two scenarios of development of the instability of slow solitons are possible, depending on initial perturbation: explosion (probably leading to further layer rupture) and splitting into pair of fast stable solitons. No other localized waves have been detected with direct numerical simulation, meaning this one-parameter family of solitons to be the only localized waves in the system. The system dynamics can be fully represented as kinetics of gas of solitons until an explosion (and away from it).

It is not possible to compare our results to the results presented by Wolf [1, 2] in detail. Wolf presented the wave patterns of the interface at the inverted state (the heavy liquid above the light one) above the linear instability threshold of the flat-interface non-inverted state. Meanwhile, we consider the waves on the interface at the non-inverted state below the threshold.

We are thankful to Dr. Maxim V. Pavlov, Dr. Takayuki Tsuchida, and two unknown reviewers for their useful comments on the paper and drawing our attention to the fact that system (34)–(35) is identical to the ‘plus’ Boussinesq equation. The work has been supported by the Russian Science Foundation (grant no. 14-21-00090).

To the memory of our teachers and friends A. A. Cherepanov, D. V. Lyubimov and S. V. Shklyaev.

- [1] Wolf G H 1961 The dynamic stabilization of the Rayleigh-Taylor instability and the corresponding dynamic equilibrium *Z. Phys.* **227** 291–300.
- [2] Wolf G H 1970 Dynamic Stabilization of the Interchange Instability of a Liquid-Gas Interface *Phys. Rev. Lett.* **24** 444.
- [3] Lyubimov D V and Cherepanov A A 1987 On the development of steady relief on fluid interface in a vibrational field *Fluid Dynamics* **21** 849–854.
- [4] Khenner M V, Lyubimov D V and Shotz M M 1998 Stability of a Fluid Interface Under Tangential Vibrations *Fluid Dynamics* **33** 318–323.
- [5] Khenner M V, Lyubimov D V, Belozerova T S and Roux B 1999 Stability of Plane-Parallel Vibrational Flow in a Two-Layer System *European Journal of Mechanics B/Fluids* **18** 1085–1101.
- [6] Zamaraev A V, Lyubimov D V and Cherepanov A A 1989 On equilibrium shapes of the interface between two fluids in vibrational field *Hydrodynamics and Processes of Heat and Mass Transfer* (Sverdlovsk: Ural Branch of Acad. of Science of USSR) p 23–26 [*in Russian*].
- [7] Goldobin D S, Kovalevskaya K V and Lyubimov D V 2014 Elastic and inelastic collisions of interfacial solitons and integrability of two-layer fluid system subject to horizontal vibrations *in preparation*.
- [8] Shklyaev S, Alabuzhev A A and Khenner M 2009 Influence of a longitudinal and tilted vibration on stability and dewetting of a liquid film *Phys. Rev. E* **79** 051603.
- [9] Benilov E S and Chugunova M 2010 Waves in liquid films on vibrating substrates *Phys. Rev. E* **81** 036302.
- [10] Thiele U, Vega J M and Knobloch E 2006 Long-wave Marangoni instability with vibration *J. Fluid Mech.* **546** 61–87.
- [11] Nepomnyashchy A A and Simanovskii I B 2013 The influence of vibration on Marangoni waves in

- two-layer films *J. Fluid Mech.* **726** 476–496.
- [12] Akylas T R 1993 Envelope solitons with stationary crests *Phys. Fluids* **5** 789–791.
  - [13] Longuet-Higgins M S 1993 Capillary-gravity waves of solitary type and envelope solitons on deep water *J. Fluid Mech.* **252** 703–711.
  - [14] Goldobin D S and Lyubimov D V 2007 Soret-Driven Convection of Binary Mixture in a Horizontal Porous Layer in the Presence of a Heat or Concentration Source *JETP* **104** 830–836.
  - [15] Watson E J 1964 The radial spread of a liquid jet over a horizontal plane *J. Fluid Mech.* **20** 481–499.
  - [16] Boussinesq J 1872 Théorie des ondes et des remous qui se propagent le long d’un canal rectangulaire horizontal, en communiquant au liquide contenu dans ce canal des vitesses sensiblement pareilles de la surface au fond *Journal de Mathématiques Pures et Appliquées. Deuxième Série* **17** 55–108.
  - [17] Choi W and Camassa R 1999 Fully nonlinear internal waves in a two-fluid system *J. Fluid Mech.* **396** 1–36.
  - [18] Manoranjan V S, Mitchell A R and Morris J L 1984 Numerical solutions of the good Boussinesq equation *SIAM J. Sci. Statist. Comput.* **5**(4) 946–957.
  - [19] Manoranjan V S, Ortega T and Sanz-Serna J M 1988 Soliton and antisoliton interactions in the “good” Boussinesq equation *J. Math. Phys.* **29**(9) 1964–1968.
  - [20] Bogdanov L V and Zakharov V E 2002 The Boussinesq equation revisited *Physica D* **165** 137–162.
  - [21] Bona J L and Sachs R L 1988 Global existence of smooth solutions and stability of solitary waves for a generalized Boussinesq equation *Comm. Math. Phys.* **118**(1) 15–29.
  - [22] Liu Y 1993 Instability of solitary waves for generalized Boussinesq equations *J. Dynam. Differential Equations* **5**(3) 537–558.